Compact approximate solution to the Friedel-Anderson impurity problem

Gerd Bergmann*
Department of Physics, University of Southern California, Los Angeles, California 90089-0484, USA

(Received 18 May 2006; revised manuscript received 21 July 2006; published 23 October 2006)

An approximate ground state of the Anderson-Friedel impurity problem is presented in a very compact form. It requires solely the optimization of two localized electron states and consists of four Slater states (Slater determinants). The resulting singlet ground-state energy lies far below the Anderson mean-field solution and agrees well with the numerical results by Gunnarsson and Schönhammer, who used an extensive $1/N_f$ expansion for a spin-$\frac{1}{2}$ impurity with double occupancy of the impurity level.

DOI: 10.1103/PhysRevB.74.144420 PACS number(s): 75.20.Hr, 72.15.Rn

I. INTRODUCTION

The formation of magnetic impurities in a metal and their properties is a fascinating field in solid state physics. Although some of the experimental anomalies were already discovered in the 1930s by de Haas *et al.*[1] it is still a subject of great interest. The work of Friedel[2] and Anderson[3] (FA) laid the foundation in the investigation of the "magnetic impurity problem." They considered a host with an s band in which a transition metal atom is dissolved. The s electrons can hop onto the d impurity via the hopping matrix element V_{sd}. The tenfold degeneracy of a real d impurity is simplified and reduced to a twofold degeneracy for spin-up and spin-down. If both states are occupied they repel each other due to the Coulomb exchange energy U. This yields the Friedel-Anderson Hamiltonian

$$H_{\mathrm{FA}} = \sum_{\sigma} \left(\sum_{\nu=1}^{N} \varepsilon_{\nu} c_{\nu\sigma}^{*} c_{\nu\sigma} + E_d d_{\sigma}^{*} d_{\sigma} + \sum_{\nu=1}^{N} V_{sd}(\nu) \times (d_{\sigma}^{*} c_{\nu\sigma} + c_{\nu\sigma}^{*} d_{\sigma}) \right) + U n_{d+} n_{d-}. \quad (1)$$

Here a finite s band with N states is used. The $c_{\nu\sigma}^{*}$ and the d_{σ}^{*} are the creation operators of the (free) s electrons and the d impurity. The d_{σ} states are assumed to be orthogonal to the s states c_{ν}^{*}.

Friedel and Anderson derived a mean-field solution for the Hamiltonian (1) which predicted which transition metal impurities form a magnetic local moment and which do not.

Kondo[4] showed that multiple scattering of conduction electrons by a magnetic impurity yields a divergent contribution to the resistance in perturbation theory. Kondo's paper stimulated a large body of theoretical and experimental work which changed our understanding of d and f impurities completely (see, for example, Refs. 5–16). A large number of sophisticated methods were applied in the following three decades to better understand and solve the Kondo and Friedel-Anderson problem. In particular, it was shown that at zero temperature the Friedel-Anderson impurity is in a nonmagnetic state. To name a few of these methods: scaling,[17] renormalization[8,18–20] Fermi-liquid theory,[21,14] slave-bosons (see, for example, Ref. 22), large-spin limit,[23,15] and the Bethe ansatz.[11,24] After decades of research exact solutions of the Kondo and Friedel-Anderson problems were derived[11,12] representing a magnificent theoretical achievement.

The exact solution does not solve all questions. It uses an s-electron band with a linear dispersion relation, extending from minus infinity to plus infinity and a constant density of states (the cutoff is only performed at the end of the calculation). Furthermore it is such a complex solution that only a limited number of parameters can be calculated and many noncritical or nondivergent contributions are neglected. For the majority of practical problems one uses approximate solutions. One particularly popular method is the large-spin method which will be discussed below.

While the single-impurity problem is intensively studied and well understood the many-impurity problem and the periodic Anderson problem are still in a rather incomplete state.[25] Any simplified treatment of the single impurity may provide a new tool to improve the treatment of the latter.

Above the Kondo temperature and for sufficient large U the Friedel-Anderson impurity shows a magnetic moment. There is a large body of research in which the magnetic moment of impurities is calculated.[26–30] Generally spin-density-functional theory is used for this task. Within this theory the electronic structure of the host and the impurity is calculated from first principles without any adjustable parameters. However, in the final step the mean-field method is applied to obtain the local magnetic moment. Although this is a zero-temperature calculation (where the impurity should be in the Kondo singlet state) it is generally argued that such a calculation yields the magnetic moment above the Kondo temperature (which, at lower temperatures, is hidden in the singlet state).

In a recent paper, Bergmann[31] introduced an approach called the AFR approach (AFR for artificial Friedel resonance) to treat the magnetic state. The calculation showed that the mean-field result for the magnetic moment of impurities is not reliable. By rewriting the mean-field ground state in a rotated basis and optimization one obtains a solution which is much lower in energy, requires a much larger critical U for the formation of a moment and yields smaller magnetic moments. And this despite the fact that the improved solution has the same structure as the mean-field solution. Since there is a large body of spin-density-functional theory calculations for magnetic impurities, a reevaluation of this method might be required.

This paper extends the AFR method to treat the singlet state ground state of the Friedel-Anderson problem. In Sec.

II the AFR method is briefly described. In Sec. III the singlet state of the Friedel-Anderson model is derived. In Sec. IV the results are discussed. In the Appendix some details of the calculation are summarized.

II. ARTIFICIAL FRIEDEL RESONANCE STATE

If one sets in Eq. (1) the Coulomb exchange interaction equal to $U=0$ then one obtains for spin-up and spin-down electrons the Friedel Hamiltonian. For an s band with a finite number N of states and an occupation number n (for each spin) one can write the (exact) ground state as an antisymmetric product of n single electrons states. Since the spin-up and spin-down components of the ground state are identical for the Friedel Hamiltonian we consider for the moment only spinless electrons. The single-electron eigenstates of the Friedel Hamiltonian are given by (in the following, single electron states are denoted by their creation operators)

$$b_j^* = \sum_\nu \beta_{j,\nu} c_\nu^* + \beta_j d^* . \tag{2}$$

Details are given in the Appendix. The exact n-electron ground state is given by

$$\Psi_{\mathrm{Fr}}^0(n) = \prod_{j=1}^{n} b_j^* \Phi_0 , \tag{3}$$

where Φ_0 is the vacuum state.

Inserting (2) into (3) yields

$$\Psi_{\mathrm{Fr}}^0(n) = \prod_{j=1}^{n} \left(\sum_\nu \beta_{j,\nu} c_\nu^* + \beta_j d^* \right) \Phi_0 = \Psi_n + \Psi_{n-1} d^* ,$$

where Ψ_n and Ψ_{n-1} are (complicated) n- and $(n-1)$-electron wave functions composed of s electrons only (see the Appendix).

On first sight it might appear surprizing that one can find a special basis $\{a_i^*\}$ with $(0 \leqslant i \leqslant N-1)$ in the s-electron Hilbert space in which Ψ_n and Ψ_{n-1} are exactly presented by

$$\Psi_{n-1} = \prod_{i=1}^{n-1} a_i^* \Phi_0 ,$$

$$\Psi_n = a_0^* \prod_{i=1}^{n-1} a_i^* \Phi_0 = \prod_{i=0}^{n-1} a_i^* \Phi_0 .$$

This exact relation can be proven by geometrical considerations in the $(N+1)$-dimensional Hilbert space of d and s electrons.[32]

A. Ground state of the Friedel Hamiltonian

In the basis $\{a_i^*\}$ the exact ground state of the Friedel Hamiltonian takes the form[33,32]

$$\Psi_{\mathrm{Fr}} = (A' a_0^* + B' d^*) \prod_{i=1}^{n-1} a_i^* \Phi_0 . \tag{4}$$

The state a_0^* is a localized state which is built from the states of the s band,

$$a_0^* = \sum_{\nu=1}^{N} \alpha_\nu^0 c_\nu^* . \tag{5}$$

The a_i^* $(1 \leqslant i \leqslant N-1)$ together with a_0^* represent a new basis. The a_i^* are orthogonal to a_0^* and to each other and their $(N-1)$ submatrix of the s-band Hamiltonian $H_0 = \Sigma \varepsilon_\nu n_\nu$ is diagonal. (The construction of the states $\{a_0^*, a_i^*\}$ is discussed in the Appendix.) The states a_i^* are uniquely determined from the state a_0^*. Their form is

$$a_i^* = \sum_{\nu=1}^{N} \alpha_\nu^i c_\nu^* . \tag{6}$$

In this new basis the Friedel Hamiltonian (for each spin) can be written as

$$H_{\mathrm{Fr}} = \sum_{i=1}^{N-1} E(i) a_i^* a_i + E(0) a_0^* a_0 + \sum_{i=1}^{N-1} V_{fr}^a(i) (a_0^* a_i + a_i^* a_0) + E_d d^* d + V_{sd}^a(0)(d^* a_0 + a_0^* d) + \sum_{i=1}^{N-1} V_{sd}^a(i)(d^* a_i + a_i^* d), \tag{7}$$

where

$$E(i) = \sum_\nu \alpha_\nu^i \varepsilon_\nu \alpha_\nu^i , \quad E(0) = \sum_\nu \alpha_\nu^0 \varepsilon_\nu \alpha_\nu^0 ,$$

$$V_{sd}^a(i) = \sum_\nu V_{sd}(\nu) \alpha_\nu^i , \quad V_{fr}^a(i) = \sum_\nu \alpha_\nu^i \varepsilon_\nu \alpha_\nu^0 . \tag{8}$$

In the Hamiltonian (7) the first three terms represent the free electron Hamiltonian. The a_0^*-state represents an artificial Friedel resonance state (AFR state). It is interesting to note that the d^* state and the localized a_0^* state in (7) are on equal footing. The AFR state a_0^* is a sister state to the state d^*.

The terms with the matrix elements $V_{fr}^a(i)$ and $V_{sd}^a(i)$ yields the hopping between $(a_i^* \leftrightarrow d^*)$ and $(a_i^* \leftrightarrow a_0^*)$. For the state $(A' a_0^* + B' d^*)$ the individual hopping matrix elements cancel each other, making Ψ_{Fr} the ground state.

B. Mean-field solution of the Friedel-Anderson Hamiltonian

Now we return to the Friedel-Anderson Hamiltonian. Anderson derived a mean-field solution for its ground state which is the product of two Friedel ground states, as given by Eq. (4), one for spin-up and one for spin-down. Therefore this mean-field solution Ψ_{mf} has the form

$$\Psi_{\mathrm{mf}} = (A_- a_{0-}^* + B_- d_-^*) \prod_{i=1}^{n-1} a_{i-}^* \Phi_0 * (A_+ a_{0+}^* + B_+ d_+^*) \prod_{i=1}^{n-1} a_{i+}^* \Phi_0 , \tag{9}$$

where

$$A_+^2 + B_+^2 = 1, \quad A_-^2 + B_-^2 = 1 . \tag{10}$$

The wave function Ψ_{mf} yields exactly the same state as Anderson's mean-field solution if one uses the correct states

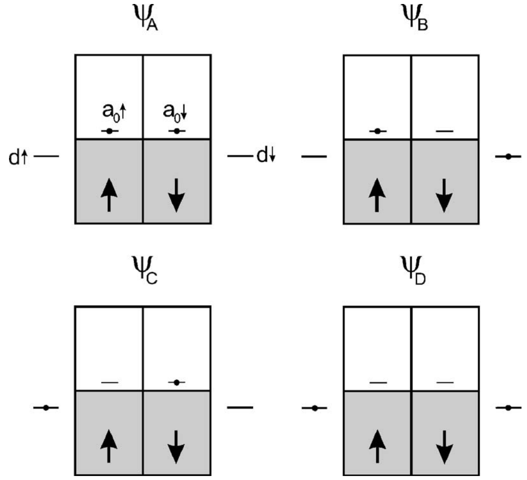

FIG. 1. The four Slater states used in the "magnetic ground state." In each component either the d^* state or the AFR state a_0^* is occupied.

a_{0+}^* and a_{0-}^* and coefficients A_+, B_+, A_-, B_-. These can be obtained by variation (see the Appendix) fulfilling the condition (10) or analytically.[32]

One can expand the two brackets of Ψ_{mf} in Eq. (9) and rewrite the state as

$$\Psi_{\text{mf}} = (Aa_{0-}^*a_{0+}^* + Bd_-^*a_{0+}^* + Ca_{0-}^*d_+^* + Dd_-^*d_+^*)\prod_{\sigma,i=1}^{n-1} a_{i\sigma}^*\Phi_0$$

$$= A\Psi_A + B\Psi_B + C\Psi_C + D\Psi_D. \tag{11}$$

If one varies in (11) the states a_{0+}^*, a_{0-}^* and A,B,C,D replacing the condition (10) by (12),

$$A^2 + B^2 + C^2 + D^2 = 1 \tag{12}$$

then one obtains a modified state. We denote this state as the (potentially) "magnetic state" Ψ_{MS}. The energy of Ψ_{MS} lies clearly below the energy of the mean-field solution Ψ_{mf}. The magnetic state Ψ_{MS} requires a much larger value of U than Ψ_{mf} to form a magnetic moment. The critical value of the Coulomb exchange energy U_{cr} is almost twice as large as in the mean-field solution.

Since in many calculations of the magnetic moment of impurities the mean-field approximation is used one must reevaluate the resulting moments. This may also apply to the impurity calculations which use the spin-density-functional theory because in the majority of these calculations the mean-field theory is used in the final analysis.

Each of the four states Ψ_A, Ψ_B, Ψ_C, and Ψ_D is normalized and they are all orthogonal to each other because they differ in the occupations of the d_+^* or d_-^* state. In Fig. 1 the four components Ψ_A, Ψ_B, Ψ_C, and Ψ_D of the state Ψ_{MS} are graphically shown.

C. The singlet state

The ground state of the Friedel-Anderson problem is symmetric in spin-up and spin-down electrons. From Ψ_{MS} one can construct a mirror state by exchanging spin-up and spin-down. Combining the two states yields then an approximate singlet state which is denoted as Ψ_{SS}. It is given by the following expression:

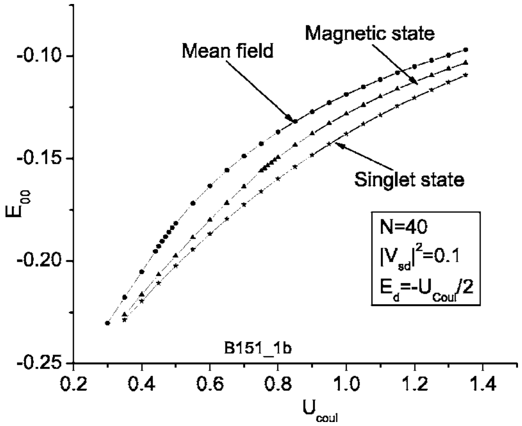

FIG. 2. A comparison between the ground-state energies of the singlet state Ψ_{SS}, the magnetic state Ψ_{MS}, and Anderson's mean-field state Ψ_{mf}.

$$\Psi_{\text{SS}} = \Psi_{\text{MS}}(\uparrow\downarrow) \mp \Psi_{\text{MS}}(\downarrow\uparrow) = (Aa_{0-\downarrow}^*a_{0+\uparrow}^* + Bd_{-\downarrow}^*a_{0+\uparrow}^*$$

$$+ Ca_{0-\downarrow}^*d_{+\uparrow}^* + Dd_{-\downarrow}^*d_{+\uparrow}^*)\prod_{i=1}^{n-1} a_{i+\uparrow}^*\prod_{i=1}^{n-1} a_{i-\downarrow}^*\Phi_0 \mp (Aa_{0-\uparrow}^*a_{0+\downarrow}^*$$

$$+ Bd_{-\uparrow}^*a_{0+\downarrow}^* + Ca_{0-\uparrow}^*d_{+\downarrow}^* + Dd_{-\uparrow}^*d_{+\downarrow}^*)\prod_{i=1}^{n-1} a_{i+\downarrow}^*\prod_{i=1}^{n-1} a_{i-\uparrow}^*\Phi_0. \tag{13}$$

The sign $\mp$ is chosen so that one obtains an (approximate) singlet state. (If one moves in each term all spin-up creation operators to the left-hand side and all spin-down creation operators to the right-hand side then the plus sign is appropriate.) This state is not normalized and the "B" and "C" components are not orthogonal to each other. This introduces some additional terms in the ground-state energy. Furthermore the matrix elements between the states $\Psi_{\text{MS}\uparrow}$ and $\Psi_{\text{MS}\downarrow}$ become determinants of single electron matrix elements. This is discussed in the Appendix.

For the numerical calculation an s band with N electron states c_ν^* is used. The energy scale is logarithmic, as introduced by Wilson[8] in his Kondo paper. The level separation becomes finer and finer when the Fermi energy $\varepsilon_F=0$ is approached. The number of states N is generally set equal to 40 and it is quoted within the figures. In the discussion [Figs. 4(a) and 4(b)] a criterion is given for checking whether N is large enough. A brief description of these electron states is given in the Appendix.

The ground-state energy of the singlet state is shown in Fig. 2 as a function of U with $E_d=-U/2$ (stars). Its energy clearly lies below the energy of the magnetic state Ψ_{MS} (up triangles). For comparison the ground-state energy of the mean-field state Ψ_{mf} is included in Fig. 2 (circles).

III. DISCUSSION

A. Comparison with the large N_f expansion

A number of approximate solutions have been suggested in the literature in which a localized electron state forms a

TABLE I. A comparision between the numerical results by Gunnarsson and Schönhammer and the author for the case of $N_f=2$. The parameters, given in the units used by GS, are $B_{GS}=6$ eV, $E_{d,GS}=-2.5$ eV, $V_{GS}=1.$ eV, $U_{GS}=5$ eV. The first column gives the states included in the large spin method, the second column gives the ground-state energy. The third, fourth, and fifth columns give the weight of zero, single, and double occupation of the d states. The sixth column gives the number of optimized parameters (amplitudes) in this calculation.

States	E_0 (Ev)	f_0	f_1	f_2	Parameters
$\|0\rangle+a+b$	−0.108	0.001	0.974	0.025	$(1/N_f)^0$
$+c+d+e$	−0.238	0.031	0.938	0.031	$(1/N_f)^1$
$+f+g$	−0.245	0.034	0.931	0.034	$(1/N_f)^2$
Singlet state	−0.239	0.035	0.931	0.034	

singlet state with the magnetic impurity, see for example, Refs. 34, 35, and 23. They have been suggested for the Kondo problem and the Friedel-Anderson model. One particularly popular approximation is the large N_f expansion (see, for example, Refs. 23 and 15). In the large N_f expansion one assumes that the impurity has a large total angular momentum J_f (J_f because this method is often used for f impurities). The "spin" has then a degeneracy of $N_f=(2J_f+1)$ of the total angular momentum states. In the limit of infinite N_f (the large N_f limit) this method yields an exact ground state. For smaller spin, in particular for spin-$\frac{1}{2}$, one generally performs an expansion in powers of $1/N_f$.

Gunnarsson and Schönhammer (GS) (Ref. 36) applied the large N_f method to a finite Coulomb interaction and spin-$\frac{1}{2}$, including double occupancy of the impurity level. They calculated the ground-state energy in different approximations. They included up to 10^7 basis states and handled the huge matrices by reducing the problem to a linear eigenvalue problem. GS give their energy parameters in units of eV. In this paper their parameters are denoted with the index GS. These parameters are one-half the bandwidth B_{GS}, the d-state energy $E_{d,GS}$, the Coulomb energy U_{GS}. For the s-d-hopping transition they use an elliptic form

$$[V(\varepsilon)]^2 g(\varepsilon) = \frac{2V_{GS}^2}{\pi B_{GS}^2}\sqrt{(B_{GS}^2-\varepsilon^2)}, \qquad (14)$$

where $g(\varepsilon)$ is the density of states (per spin). All these parameters are energies or potentials. By dividing these energy parameters by B_{GS} one obtains the appropriate parameters for the present calculation. When the numerical calculation is completed the resulting ground-state energy must be multiplied with B_{GS} for a comparison with the GS results.

Gunnarsson and Schönhammer calculated in Ref. 36 the ground-state energy (for $N_f=2$) with the following parameters: $B_{GS}=6$ eV, $U_{GS}=5$ eV, $E_{d,GS}=-2.5$ eV. They performed two calculations, one for $V_{GS}=1$ eV and another for $V_{GS}=2$ eV. The results are shown in Tables I and II. The first column gives the electron states used in the calculation (for details see Ref. 36 and the Appendix). The second column gives the calculated ground-state energies. In the third, fourth, and fifth columns the symbols f^0, f^1, f^2 give the probabilities for a d occupation of 0,1,2. The last column gives the power of the $(1/N_f)$ expansion. The last row gives the results of the present calculation for the singlet state. The values for f_0, f_1, f_2 agree perfectly. Also the ground-state energies are quite close with $E_{GS}=-0.245$ eV and $E_0=-0.239$ eV of the present calculation.

For $V_{GS}=2$ eV the ground-state energy of the present calculation lies even below the value of the $1/N_f$ expansion, as shown in Table II.

The state g requires the variation of more than 15^6, i.e., more than 10^7 amplitudes. In the present calculation the singlet state requires the variation of $2N=60$ amplitudes. Keeping this in mind, the resulting ground state of the present calculation is rather compact.

B. Properties of the artificial Friedel resonance state

The states a_{0+}^* and a_{0-}^* are of particular importance of the present treatment of the Friedel-Anderson impurity. They determine the rotation of the s-electron basis in Hilbert space and therefore the solution of the problem. We analyze the composition of $a_{0\pm}^*$ in terms of the original s-state energies

TABLE II. A comparision between the numerical results by Gunnarsson and Schönhammer and this papper for the case of $V_{GS}=2$ eV. Everything else is identical to Table I.

States	E_0 (eV)	f_0	f_1	f_2	Expansion
$\|0\rangle+a+b$	−0.628	0.141	0.778	0.081	$(1/N_f)^0$
$+c+d+e$	−1.126	0.140	0.745	0.115	$(1/N_f)^1$
$+f+g$	−1.217	0.137	0.732	0.132	$(1/N_f)^2$
Singlet state	−1.234	0.140	0.722	0.138	

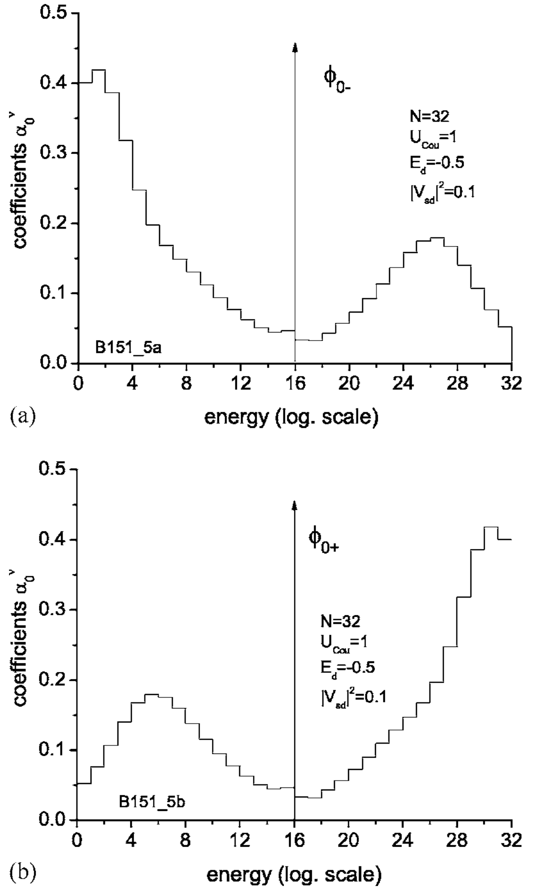

FIG. 3. (a), (b) The coefficients α_0^ν for the AFR states a_{0+}^* and a_{0-}^*. The Wilson spectrum is used (for the region on the left-hand side of the arrow the numbers ν corresponds to an energy of $E_\nu=-1/2^\nu$, on the right-hand side to $E_\nu=+1/2^{N-\nu}$). The energy of the s electron c_ν^* is $(E_\nu+E_{\nu-1})/2$.

ε_ν. As discussed above, $a_{0\pm}^*$ is composed of the original s-basis c_ν^* with the amplitudes $\alpha_{\nu\pm}^0$,

$$a_{0\pm}^* = \sum_{\nu=1}^{N} \alpha_{\nu\pm}^0 c_{\nu\pm}^* .$$

In Figs. 3(a) and 3(b) the coefficients $\alpha_{\nu+}^0$ and $\alpha_{\nu-}^0$ of the states a_{0+}^* and a_{0-}^* are plotted for the parameters: $U_{\mathrm{Coul}}=1$, $E_d=-0.5$, $|V_{sd}|^2=0.1$ and the number of s states is $N=32$. One recognizes that the amplitudes at large absolute energies are very different for spin-up and spin-down. They are almost mirror images.

This difference in the amplitudes of a_{0+}^* and a_{0-}^* indicates that the singlet state is composed of magnetic substates, i.e., the states $\Psi_{\mathrm{MS}}(\uparrow\downarrow)$ and $\Psi_{\mathrm{MS}}(\downarrow\uparrow)$ in Eq. (13) have opposite finite moments. This can be understood in the following sequence of reasoning:

(i) Since the energies $E_\pm(0)$ are given by $E_\pm(0)=\Sigma_\nu|\alpha_{\nu,\pm}^0|^2\varepsilon_\nu$ [see Eq. (8)] one recognizes that $E_-(0)<0$ and $E_+(0)>0$. [Here one must keep in mind that we have a logarithmic scale. The four amplitudes on the right-hand side of Fig. 3(a) or Fig. 3(b) (i.e., $\alpha_{29}^0,\ldots,\alpha_{32}^0$) cover the energy range from $+\frac{1}{16}$ to $+1$, i.e., 93% of the positive energy range while $\alpha_1^0,\ldots,\alpha_4^0$ cover 93% of the negative energy range.]

(ii) For the simple Friedel impurity problem the author observed that the energy $E(0)$ of the AFR state a_0^* has the opposite sign as the d^* state energy. For $E_d<0$ this yields a larger occupation of the d^* state in Eq. (4) [in $(A'a_0^*+B'd^*)$ one finds $|B'|^2>|A'|^2$] and vice versa.

(iii) The mean-field Hamiltonian of the Friedel-Anderson model is, for each spin direction, equivalent to a Friedel impurity with an effective d^* state energy of $E_{d,\sigma}=(E_d+U\langle n_{d,-\sigma}\rangle)$. In the magnetic solution the occupations of the $d_\uparrow^*$ and $d_\downarrow^*$ states and the energies $E_{d\uparrow}$ and $E_{d\downarrow}$ are different. For the symmetric case $(E_d=-U/2)$ this yields opposite d^* state energies, $E_{d\uparrow}=-E_{d\downarrow}$. The corresponding AFR states $a_{0\uparrow}^*$ and $a_{0\downarrow}^*$ have therefore also opposite energies.

(iv) Although the present solution goes beyond the mean-field solution the composition of the AFR states indicates that the substates $\Psi_{\mathrm{MS}}(\uparrow\downarrow)$ and $\Psi_{\mathrm{MS}}(\downarrow\uparrow)$ in Eq. (13) are asymmetric in spin-up and spin-down and each one possesses a magnetic moment.

For the analysis at small energies we plot the occupation density $|\alpha_{0\pm}^\nu|^2/(E_\nu+E_{\nu-1})$ as a function of ν. In Figs. 4(a) and 4(b) these densities are shown for $N=32$ and $N=48$. In the latter case the energy interval next to the arrow (zero energy) is $1/2^8$ times smaller than for the lower plot. Obviously the subdivision at the Fermi energy is not yet sufficiently small at the lower plot for $N=32$.

While amplitudes and occupations for large energies were rather different for a_{0+}^* and a_{0-}^* the occupation at small energies is almost identical. This is shown in Fig. 5 where the occupations of a_{0+}^* and a_{0-}^* are plotted in the same figure. At energies close to the Fermi energy the occupation of a_{0+}^* and a_{0-}^* are essentially identical. On a linear energy scale at small energies the plots in Fig. 4(b) and Fig. 5 are essentially identical.

The average occupation density of the states a_{0+}^* and a_{0-}^* is 1/2 since the band ranges form -1 to $+1$. Therefore a density of more than 100 is quite large.

The AFR states have weight at small and large energies. The weight at large energies is responsible for the large "perturbative" part of the ground-state energy. The weight at small energies is responsible for the anomalous behavior at low temperatures, the Kondo effect.

IV. CONCLUSIONS

This paper suggests a very compact approximate ground state for the Friedel-Anderson impurity. Its center piece are two artificial resonance states a_{0+}^*,a_{0-}^* for the spin-up and spin-down s electrons. These are combined with the d electrons for spin-up and spin-down d_+^*,d_-^* into two-electron states of total spin zero, i.e., $(Aa_{0-}^*a_{0+}^*+Bd_-^*a_{0+}^*+Ca_{0-}^*d_+^*+Dd_-^*d_+^*)$. Then for each spin a new s-electron basis $\{a_{i\pm}^*\}$ is built. These two bases are completely determined by the AFR states. Finally the $(n-1)$ lowest states of the two basis are occupied yielding the s-electron background $\Pi_{i=1,\sigma}^{n-1}a_{i\sigma}^*\Phi_0$. The compositions of the AFR states a_{0+}^*,a_{0-}^* are calculated

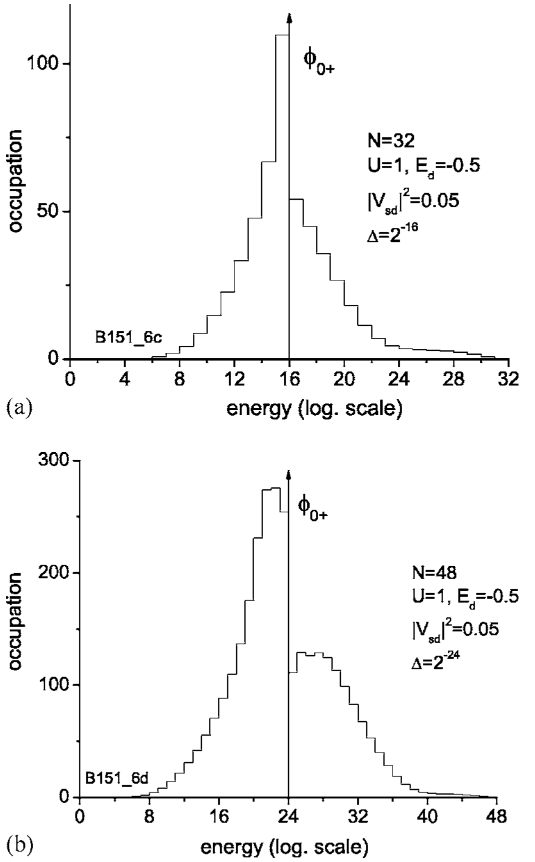

FIG. 4. (a), (b) The low energy occupation in the state a_{0+}^{*} for different subdivision of the energy close to the Fermi energy. In (a) the smallest subdivision is $\Delta = 2^{-16} \approx 1.5 \times 10^{-5}$ and in (b) it is $\Delta = 2^{-24} \approx 6 \times 10^{-8}$. While in the upper plot Δ is not yet small enough, one observes on the lower plot the occupation of a_{0+}^{*} has saturated.

by numerical variation which rotates the s-electron bases in Hilbert space. This ansatz is exact for a spin degeneracy N_f of "1" and infinity.

The properties of the singlet state are investigated. Its ground-state energy and the occupations f_0, f_1, f_2 of the d states are in very good agreement with the extensive calculations by Gunnarsson and Schönhammer using the large N_f expansion. However, while in the large N_f expansion one must go to a large basis of states to obtain a good ground-state energy the present solution is extremely compact.

The spectral composition of the two AFR states is quite interesting. Their composition is quite different away from the Fermi energy. Close to the Fermi energy one finds a large peak in the occupation density which saturates only for very small energies. This low energy occupation is essentially identical for the spin-up and the spin-down AFR state.

A detailed analysis of the present solution is planned. For example, the construction of the triplet state and the calculation of transport scattering by the impurity in this ground state are desirable. Above all, it is of interest whether an extension of the presented solution can contribute to the periodic Anderson impurity problem.

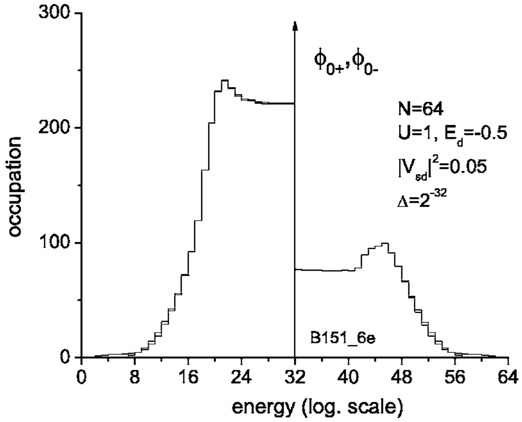

FIG. 5. The occupation of the spin-up and spin-down AFR states for $N=64$. Note that the figure shows two curves as a function of ν $(0 \leqslant \nu \leqslant 64)$. At small energies (close to the center arrow) the two are almost identical. (The difference between Φ_{0+} and Φ_{0-} is of the order of the width of the curve.)

APPENDIX

Friedel's resonance Hamiltonian

The Friedel Hamiltonian has the form

$$H_{\mathrm{Fr}} = \sum_{\nu=1}^{N} \varepsilon_{\nu} c_{\nu}^{*} c_{\nu} + E_d d^{*} d + \sum_{\nu=1}^{N} V_{sd}(\nu)(d^{*} c_{\sigma} + c_{\sigma}^{*} d). \tag{A1}$$

The single-electron eigenstates b_j^{*} of the Friedel Hamiltonian consist of a superposition of all s states plus the d state,

$$b_j^{*} = \sum_{\nu} \beta_{j,\nu} c_{\nu}^{*} + \beta_j d^{*}. \tag{A2}$$

The coefficients are given in terms of the new eigenenergies E_j,

$$\beta_j = \left(1 + \sum_{\nu=1}^{N} \frac{|V_{sd}(\nu)|^2}{(E_j - \epsilon_{\nu})^2} \right)^{-1/2},$$

$$\beta_{j,\nu} = \beta_j \frac{V_{sd}(\nu)}{(E_j - \epsilon_{\nu})}.$$

The latter are determined by the implicit relation,

$$E_j = E_d + \sum_{\nu=1}^{N} \frac{|V_{sd}(\nu)|^2}{E_j - \epsilon_{\nu}}.$$

The n-electron ground state is simply the product of the n lowest single electron states,

$$\Psi_{\mathrm{Fr}}^{0}(n) = \prod_{j=1}^{n} b_j^{*} \Phi_0, \tag{A3}$$

where Φ_0 is the vacuum state. Inserting (A2) into (A3) yields

$$\Psi^0_{\mathrm{Fr}}(n) = \prod_{j=1}^{n}\left(\sum_{\nu}\beta_{j,\nu}c^*_\nu + \beta_j d^*\right)\Phi_0 = \prod_{j=1}^{n}\left(\sum_{\nu}\beta_{j,\nu}c^*_\nu\right)\Phi_0$$

$$+ d^*\sum_j \beta_j \prod_{\substack{j'=1\\ j'\neq j}}^{n}\left(\sum_\nu \beta_{j',\nu}c^*_\nu\right)\Phi_0 = \Psi_n + \Psi_{n-1}d^*.$$

In the special basis $\{a^*_i\}$ the n-electron eigenstate of the Friedel Hamiltonian can be written as

$$\Psi^0_{\mathrm{Fr}}(n) = (A' a^*_0 + B' d^*)\prod_{i=1}^{n-1} a^*_i \Phi_0.$$

Wilson's *s*-electron basis

Wilson[8] in his Kondo paper considers an s band with energy values ranging from -1 to 1. In the next step Wilson replaced the continuum of s states by a discrete set of states. This is done on a logarithmic scale. The discrete energy values are 1, $1/\Lambda$, $1/\Lambda^2$, etc., and -1, $-1/\Lambda$, $-1/\Lambda^2$, etc., where Λ is a parameter larger than one. (In this paper $\Lambda=2$ is chosen.) These discrete ξ_ν points are used to define a sequence of intervals: the interval ν (for $\nu<N/2$) is $\xi_{\nu-1}=-1/2^{\nu-1} < \varepsilon < -1/2^\nu = \xi_\nu$ [there are equivalent intervals for positive ξ values where ν is replace by $(N-\nu)$ but we discuss here only the negative energies]. The new Wilson states c^*_ν are a superposition of all states in the energy interval $(\xi_{\nu-1},\xi_\nu)$ and have an (averaged) energy $(\xi_\nu+\xi_{\nu-1})/2=\left(-\frac{3}{2}\right)\frac{1}{2^\nu}$, i.e., $-\frac{3}{4},-\frac{3}{8},-\frac{3}{16},\ldots,-\frac{3}{2\times 2^{N/2}},-\frac{1}{2\times 2^{N/2}}$. This spectrum continues symmetrically for positive energies.

The matrix elements $V_{sd}(\nu)$ are proportional to the amplitudes of the states c^*_ν at the origin and given by $V_{sd}(\nu) = \sqrt{(\xi_\nu-\xi_{\nu-1})/2}V^0_{sd}$. Therefore this choice of s^* states yields a dependence of the s-d matrix element $V_{sd}(\nu)$ on the state ν. One obtains the sum rule $\Sigma_{\nu=1}^N |V_{sd}(\nu)|^2 = |V^0_{sd}|^2$.

The essential advantage of the Wilson basis is that it has an arbitrarily fine energy spacing at the Fermi energy.

Construction of the basis a^*_0, a^*_i

For the construction of the state a^*_0 and the rest of the basis a^*_i one starts with the s-band electrons $\{c^*_\nu\}$ which consists of N states (for example, Wilson's states). The d^* state is ignored for the moment.

In step (1) one forms a normalized state a^*_0 out of the s states with

$$a^*_0 = \sum_{\nu=1}^{N}\alpha^0_\nu c^*_\nu. \tag{A4}$$

The coefficients α^0_ν can be at first arbitrary. One reasonable choice is $\alpha^0_\nu = 1/\sqrt{N}$.

In step (2) $(N-1)$ new basis states a^*_i $(1\leqslant i\leqslant N-1)$ are formed which are normalized and orthogonal to each other and to a^*_0.

In step (3) the s-band Hamiltonian H_0 is constructed in this new basis. One sets the state a^*_0 at the top so that its matrix elements are H_{0i} and H_{i0}.

In step (4) the $(N-1)$-sub-Hamiltonian which does not contain the state a^*_0 is diagonalized. The resulting Hamilton matrix for the s band then has the form

$$H_0 = \begin{pmatrix} E(0) & V_{fr}(1) & V_{fr}(2) & \cdots & V_{fr}(N-1) \\ V_{fr}(1) & E(1) & 0 & \cdots & 0 \\ V_{fr}(2) & 0 & E(2) & \cdots & 0 \\ \cdots & \cdots & \cdots & \cdots & \cdots \\ V_{fr}(N-1) & 0 & 0 & \cdots & E(N-1) \end{pmatrix}. \tag{A5}$$

The creation operators of the new basis are given by a new set of $\{a^*_i\}$ $(0<i\leqslant N-1)$. Again the a^*_i can be expressed in term of the s states; $a^*_i = \Sigma_{\nu=1}^N \alpha^i_\nu c^*_\nu$. After the state a^*_0 is constructed the other states a^*_i are uniquely determined. The additional s-d hopping Hamiltonian can be expressed in the terms of the new basis and one obtains the Friedel Hamiltonian as given in Eq. (7). The state Ψ_{SS} is formed and the energy expectation value (of the full Hamiltonian) is calculated.

In the final step (5) the state a^*_0 is rotated in the N-dimensional Hilbert space. In each cycle the state a^*_0 is rotated in the $(a^*_0, a^*_{i_0})$ plane by an angle θ_{i_0} for $1\leqslant i_0 \leqslant N-1$. Each rotation by θ_{i_0} yields a new $\overline{a_0}^*$,

$$\overline{a_0}^* = a^*_0 \cos\theta_{i_0} + a^*_{i_0}\sin\theta_{i_0}.$$

The rotation leaves the whole basis $\{a^*_0, a^*_i\}$ orthonormal. Step (4), the diagonalization of the $(N-1)$-sub-Hamiltonian, is now much quicker because the $(N-1)$-sub-Hamiltonian is already diagonal with the exception of the i_0 row and the i_0 column. For each rotation plane $(a^*_0, a^*_{i_0})$ the optimal a^*_0 with the lowest energy expectation value is determined. This cycle is repeated until one reaches the absolute minimum of the energy expectation value. In the example of the Friedel resonance Hamiltonian this energy agrees numerically with an accuracy of 10^{-15} with the exact ground-state energy of the Friedel Hamiltonian.[33] For the Friedel-Anderson impurity the procedure is stopped when the expectation value changes by less than 10^{-10} during a full cycle.

The effective *s*-*d* matrix element for the multielectron states

The calculation of the energy expectation value requires the calculation of many-electron matrix elements in different bases. We sketch here an example. We consider the more general case that we have two wave functions $\Psi_A = a^*_{0-}a^*_{0+}\Pi_{i=1,\sigma}^{n-1}a^*_{i\sigma}\Phi_0$ and $\Psi_B = b^*_{0-}d^*_+\Pi_{i=1,\sigma}^{n-1}b^*_{i\sigma}\Phi_0$. Each is built from two different bases: $\{a_{0+},a_{i+}\},\{a_{0-},a_{i-}\}$ and $\{b_{0+},b_{i+}\},\{b_{0-},b_{i-}\}$ (only within this section the operators b^*_0, b^*_i are used for the AFR states to distinguish the different basis systems). The energy expectation value contains for example a matrix element of the form $\langle\Psi_B|H^+_{sd}|\Psi_A\rangle$. Here the s-d Hamiltonian H^+_{sd} can be expressed in any basis but for this matrix element the a^*_{0+} representation is the optimal one. For the above matrix element one needs only the hopping for spin-up (+),

TABLE III. Gunnarsson and Schönhammer states.

Name of state	Power of expansion	occupancy of d states	s band	Number of parameters
$\vert 0\rangle$	$(1/N_f)^0$	Empty d states	Half occupied band for spin ↑ and ↓	0
a	$(1/N_f)^0$	1 $d\uparrow$ or $d\downarrow$	One ↑ or ↓ hole in $\vert 0\rangle$	$N/2$
b	$(1/N_f)^0$	2 d states	↑ hole and ↓ hole in $\vert 0\rangle$	$\alpha(N/2)^2$
c	$(1/N_f)^1$	Empty d states	One ↑ or ↓ electron-hole pair in $\vert 0\rangle$	$\alpha(N/2)^2$
d	$(1/N_f)^1$	1 $d\uparrow$ or $d\downarrow$	Two holes in $\vert 0\rangle$ and one electron	$\alpha(N/2)^3$
e	$(1/N_f)^1$	2 d states	Three holes in $\vert 0\rangle$ and one electron	$\alpha(N/2)^4$
f	$(1/N_f)^2$	Empty d states	Two ↑ or ↓ electron-hole pairs in $\vert 0\rangle$	$\alpha(N/2)^4$
g	$(1/N_f)^2$	1 $d\uparrow$ or $d\downarrow$	Three holes in $\vert 0\rangle$ and two electrons	$\alpha(N/2)^5$
h	$(1/N_f)^2$	2 d states	Four holes in $\vert 0\rangle$ and two electrons	$\alpha(N/2)^6$

$$H_{sd}^{+}=\sum_{i=0}^{N-1} V_{sd}^{a+}(i)(d_{+}^{*}a_{i+}+a_{i+}^{*}d_{+}),$$

$$V_{sd}^{a+}(i)=\sum_{\nu} V_{sd}(\nu)\alpha_{\nu+}^{i}. \tag{A6}$$

The only term in H_{sd}^{+} which yields a nonvanishing contribution to $\langle V_{sd}^{AB}\rangle$ is $\langle\Psi_B|\Sigma_{i=0}^{N-1}V_{sd}^{a+}(i)d_{+}^{*}a_{i+}|\Psi_A\rangle$.

This matrix element contains

(a) the multiscalar product of the two n electron states for spin-down $F^{AB}=\langle b_{0-}^{*}\Pi_{i=1}^{n-1}b_{i-}^{*}\Phi_0|a_{0-}^{*}\Pi_{i=1}^{n-1}a_{i-}^{*}\Phi_0\rangle$ and

(b) the matrix element $M_{sd}^{AB}=\langle d_{+}^{*}\Pi_{i=1}^{n-1}b_{i+}^{*}\Phi_0|\Sigma_{i=0}^{N-1}V_{sd}^{a+}(i)d_{+}^{*}a_{i+}|a_{0+}^{*}\Pi_{i=1}^{n-1}a_{i+}^{*}\Phi_0\rangle$.

The multiscalar product is a determinant of order n containing the single electron scalar products between all occupied states,

$$F^{AB}=\begin{vmatrix} \langle b_{0-}^{*}|a_{0-}^{*}\rangle & \langle b_{0-}^{*}|a_{1-}^{*}\rangle & \cdots & \langle b_{0-}^{*}|a_{(n-1)-}^{*}\rangle \\ \langle b_{1-}^{*}|a_{0-}^{*}\rangle & \langle b_{1-}^{*}|a_{1-}^{*}\rangle & \cdots & \langle b_{1-}^{*}|a_{(n-1)-}^{*}\rangle \\ \cdots & \cdots & \cdots & \cdots \\ \langle b_{(n-1)-}^{*}|a_{0-}^{*}\rangle & \langle b_{(n-1)-}^{*}|a_{1-}^{*}\rangle & \cdots & \langle b_{(n-1)-}^{*}|a_{(n-1)-}^{*}\rangle \end{vmatrix}. \tag{A7}$$

When the two AFR states are identical then the underlying matrix becomes the unity matrix.

Part (b) yields

$$\langle M_{sd}^{AB}\rangle=\begin{vmatrix} V_{sd}^{a+}(0) & V_{sd}^{a+}(1) & \cdots & V_{sd}^{a+}(n-1) \\ \langle b_{1+}^{*}|a_{0+}^{*}\rangle & \langle b_{1+}^{*}|a_{1+}^{*}\rangle & \cdots & \langle b_{1+}^{*}|a_{(n-1)+}^{*}\rangle \\ \cdots & \cdots & \cdots & \cdots \\ \langle b_{(n-1)+}^{*}|a_{0+}^{*}\rangle & \langle b_{(n-1)+}^{*}|a_{1+}^{*}\rangle & \cdots & \langle b_{(n-1)+}^{*}|a_{(n-1)+}^{*}\rangle \end{vmatrix}. \tag{A8}$$

Details of the comparison with the Gunnarsson and Schönhammer numerical evaluation

Gunnarsson and Schönhammer (GS) (Ref. 36) applied the large N_f method to finite Coulomb interaction and spin-$\frac{1}{2}$. They calculated the ground-state energy in different approximations. Since it is interesting to compare their results with the present calculation this paper briefly sketches the different states they considered. The corresponding graphical sketch of these states can be found in Fig. 1 of Ref. 36. These states are collected in Table III. The first column gives the GS code for the state, the second column shows in which power of the $1/N_f$ expansion the state occurs, the third column gives the occupation of the d level in the considered state, the fourth column the number of holes and electrons (above the Fermi energy) in the s band, and finally the fifth column gives the number of amplitudes (parameters) which one must optimize in the numerical evaluation (again N is the number of band states in the numerical evaluation). As an example the state d is part of the $(1/N_f)^1$ expansion, it has, for example, the $d\uparrow$ state occupied, the s band has one hole in the $s\uparrow$ band, another electron-hole pair is either in the $s\uparrow$ or $s\downarrow$ band. The total multiplicity of the state d is therefore $2\times(N/2)\times 2(N/2)^2$. The prefactor 2×2 is replaced by "α" in column 5 ($\alpha\geqslant 1$).

GS use a (different) exponential energy mesh of the form $\varepsilon_i=\pm[\alpha-\exp(x_i)]$. They use the value $\alpha=0.2$, and x_i lies in the range $[\ln(\alpha),\ln(\alpha+B_{\mathrm{GS}})]=(-1.6094,1.8245)$. This means x_i takes the values $x_i=\ln(\alpha)+i/N*[\ln(\alpha+B_{\mathrm{GS}})-\ln(\alpha)]$. GS used for N the values 9, 19, 29 and extrapolated to $N\rightarrow\infty$. For this comparison we use the corresponding energy mesh and extrapolation. The only difference is that the calculation in this paper the ε_i yield the energy frame and the energy states lie in the center between two ε_i whereas GS used the ε_i as their energy states. After the extrapolation towards $N\rightarrow\infty$ this difference should be negligible.

The energy dependent s-d matrix element $V(\varepsilon)$ adds a complication in the numerical evaluation. It varies strongly with energy. Here, we average $[V(\varepsilon)]^2$ over each energy range.

*Electronic address: bergmann@usc.edu

[1] W. J. de Haas, J. H. de Boer, and G. J. van den Berg, Physica (Amsterdam) **1**, 1115 (1934).

[2] J. Friedel, Philos. Mag. **43**, 153 (1952); Adv. Phys. **3**, 446 (1954); Philos. Mag., Suppl. **7**, 446 (1954); Can. J. Phys. **34**, 1190 (1956); Nuovo Cimento, Suppl. **7**, 287 (1958); J. Phys. Radium **19**, 38 (1958).

[3] P. W. Anderson, Phys. Rev. **124**, 41 (1961).

[4] J. Kondo, Prog. Theor. Phys. **32**, 37 (1964).

[5] M. D. Daybell and W. A. Steyert, Rev. Mod. Phys. **40**, 380 (1968).

[6] A. J. Heeger, in *Solid State Physics*, edited by F. Seitz, D. Turnbull, and H. Ehrenreich (Academic, New York, 1969), Vol. 23, p. 284.

[7] M. B. Maple, in *Magnetism*, edited by G. T. Rado and H. Suhl (Academic, New York, 1973), Vol. V, p. 289.

[8] K. G. Wilson, Rev. Mod. Phys. **47**, 773 (1975).

[9] P. W. Anderson, Rev. Mod. Phys. **50**, 191 (1978).

[10] G. Gruener and A. Zavadowski, Prog. Low Temp. Phys. **7B**, 591 (1978).

[11] P. B. Wiegmann, in *Quantum Theory of Solids*, edited by I. M. Lifshits (MIR, Moscow, 1982), p. 238.

[12] N. Andrei, K. Furuya, and J. H. Lowenstein, Rev. Mod. Phys. **55**, 331 (1983).

[13] P. Coleman, J. Magn. Magn. Mater. **47**, 323 (1985).

[14] P. Nozieres, Ann. Phys. (Paris) **10**, 19 (1985).

[15] N. E. Bickers, Rev. Mod. Phys. **59**, 845 (1987).

[16] A. C. Hewson, *The Kondo Problem to Heavy Fermions* (Cambridge University Press, Cambridge, 1993).

[17] P. W. Anderson, J. Phys. C **3**, 2436 (1970).

[18] H. O. Frota and L. N. Oliveira, Phys. Rev. B **33**, 7871 (1986).

[19] H. R. Krishna-murthy, J. W. Wilkins, and K. G. Wilson, Phys. Rev. B **21**, 1003 (1980).

[20] H. R. Krishna-murthy, J. W. Wilkins, and K. G. Wilson, Phys. Rev. B **21**, 1044 (1980).

[21] P. Nozieres, J. Low Temp. Phys. **17**, 31 (1974).

[22] D. M. Newns and N. Read, Adv. Phys. **36**, 799 (1987).

[23] O. Gunnarsson and K. Schönhammer, Phys. Rev. B **28**, 4315 (1983).

[24] P. Schlottmann, Phys. Rep. **181**, 1 (1989).

[25] P. Thalmeier and G. Zwicknagl, *Handbook on the Physics and Chemistry of Rare Earths* (Elsevier, New York, 2005).

[26] S. K. Kwon and B. I. Min, Phys. Rev. Lett. **84**, 3970 (2000).

[27] B. R. Sahu and L. Kleinman, Phys. Rev. B **67**, 094424 (2003).

[28] M. E. McHenry, J. M. MacLaren, D. D. Vvendensky, M. E. Eberhart, and M. L. Prueitt, Phys. Rev. B **40**, 10111 (1989).

[29] R. Podloucky, R. Zeller, and P. H. Dederichs, Phys. Rev. B **22**, 5777 (1980).

[30] V. I. Anisimov and P. H. Dederichs, Solid State Commun. **84**, 241 (1992).

[31] G. Bergmann, Phys. Rev. B **73**, 092418 (2006).

[32] G. Bergmann, Eur. Phys. J. B **2**, 233 (1998).

[33] G. Bergmann, Z. Phys. B: Condens. Matter **102**, 381 (1997).

[34] K. Yosida, Phys. Rev. **107**, 396 (1957).

[35] J. A. Appelbaum and J. Kondo, Phys. Rev. **170**, 542 (1968).

[36] O. Gunnarsson and K. Schönhammer, Phys. Rev. B **31**, 4815 (1985).